Available online at www.sciencedirect.com

SCIENCE DIRECT®

International Journal of Coal Geology 59 (2004) 121–136

International Journal of COAL GEOLOGY

www.elsevier.com/locate/ijcoalgeo

Integrating satellite remote sensing techniques for detection and analysis of uncontrolled coal seam fires in North China

Stefan Voigt[a,*], Anke Tetzlaff[a], Jianzhong Zhang[a], Claudia Künzer[a], Boris Zhukov[a], Günter Strunz[a], Dieter Oertel[a], Achim Roth[a], Paul van Dijk[b], Harald Mehl[a]

[a] *German Aerospace Center (DLR), Germany*
[b] *ITC, The Netherlands*

Received 27 May 2003; accepted 3 December 2003
Available online 23 April 2004

Abstract

China is the biggest producer of coal in the world and mines about 1000 Mt of raw coal per year. Approximately 70% of China's energy consumption is covered by coal. At the same time, it is estimated that about 20 Mt of coal are being burnt in uncontrolled coal fires in China each year. Because these coal fires are spread out over the whole northern part of the country, stretching from Xinjiang province in the West to the Pacific coast in the East, it is extremely difficult to keep an overview of the development of known fires as well as of newly developing ones.

Satellite remote sensing offers a powerful tool to observe and monitor such large regions; however, special methods and techniques have to be derived to accurately detect and monitor near surface coal seam fires. In this paper, an integrated satellite remote sensing approach is described allowing detection and monitoring of near surface coal seam fires by observing subtle land surface changes induced by the fires. These changes include thermal surface anomalies, changes in spectral surface characteristics as well as land subsidence caused by the fires. The methods comprise the radar interferometric generation of digital elevation models (DEMs) for geometric referencing and orthorectification of satellite imagery, dedicated analysis of thermal satellite data (daytime and nighttime), and multispectral analysis of land surface properties as well as the mapping of small-scale land subsidence by means of differential radar interferometry. It is shown how different satellite remote sensing methods can be synergistically combined to detect, analyze, and monitor near surface coal seam fires in arid or semiarid areas of North China. First results show the successful application of the methods and, furthermore, a comparison with ground measurements is given. While thermal and optical analysis of the fires can be considered robust methods, the assessment of coal seam fires using differential radar interferometry still has to be further developed in order to serve as a reliable analysis and monitoring tool. Within this work, a special focus is given to aspects of automation of the coal fire detection and analysis by means of satellite remote sensing in order to allow fire mapping in large areas with only minimal operator interaction.

Keywords: Coal fires; Remote sensing; Radar interferometry; Detection; Monitoring; Satellite

1. Introduction

China is the biggest producer of coal in the world mining about 1000 Mt of raw coal per year and

* Corresponding author. Tel.: +49-8153-28-3678; fax: +49-8153-28-1445.
E-mail address: stefan.voigt@dlr.de (S. Voigt).

0166-5162/$ - see front matter © 2004 Elsevier B.V. All rights reserved.
doi:10.1016/j.coal.2003.12.013

approximately 70% of China's energy consumption is covered by coal. According to the 10th 5-year plan (2001–2005) of the State Economic and Trade Commission for the coal industry, coal will continue to be the major source of energy for China's industries in the next 5 years. Taking into account economic growth rates of 7–8% in the coming years, it is obvious that coal is going to play an even more important role in China's economic development.

It is estimated that about 20 Mt of coal are being burnt in uncontrolled coal fires in China each year, which corresponds to about two-thirds of the yearly production of coal in Germany (approx. 30 Mt). Approximately 10 times more, about 200–300 Mt of coal, are lost in China each year, because the fires hinder the accessibility for mining operations in their surroundings. The rapid expansion of uncontrolled small-scale coal mining activities during the last 30–40 years is expected to have contributed to the increased problem of uncontrolled coal seam fires in China. Beyond the huge economic losses resulting from uncontrolled combustion of high-quality coal deposits, another problem is the enormous environmental stress that results from coal fires. Large amounts of toxic and greenhouse gases, such as SO_2, NO, CO, CH_4 and CO_2, are emitted from the fires polluting the atmosphere. Chinese coal fires alone are estimated, to emit a yearly amount of about 66 Mt of CO_2 equivalent, which equals about 0.3% of global human-induced CO_2 emissions. Within this study, it is shown how spaceborne remote sensing techniques can successfully be combined to detect, analyze, and monitor near-surface and surface coal seam fires, often occurring in very remote areas of northern China, which are difficult to access.

2. Location and geological overview

Two coal fields in the Ningxia Autonomous Region and Inner Mongolia Autonomous Region (Rujigou Coal Field and Wuda Coal Field) and two coal fields in the Xinjiang Autonomous Region (Ke-er Jian Coal Field and Tielieke Coal Field) were selected as primary study areas. The location of the study areas is shown in Fig. 1. The two coal fields in Ningxia/Inner Mongolia belong to different geological strata.

The Rujigou Coal Field (latitudes 39°00′ to 39°01′, longitude 106°03′ to 106°11′) is situated in the Helan Mountains at elevations between 1800 and 2500 m above sea level (asl). The coal-bearing layers (Yan'an Formation) of the Rujigou Coal Field were

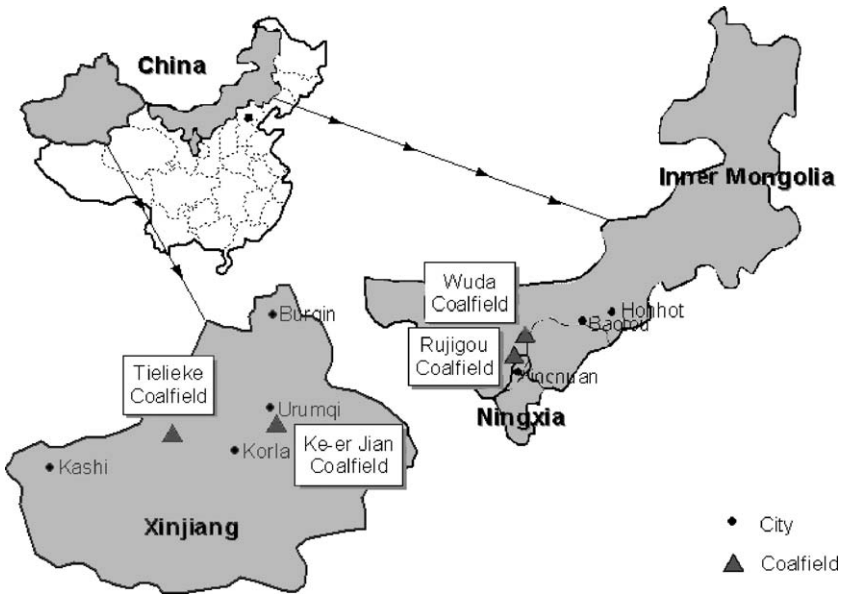

Fig. 1. Location map of the study areas in China.

deposited in a Middle Jurassic continental basin in a lacustrine-fluvial environment. The Rujigou area belongs to a wide NE–SW striking synclinorial structure. Within the 15-km-long and 8-km-wide coal field, 10 coal layers with an average cumulative thickness of 20 m are reported. The coal rank is very high, ranging from low volatile bituminous to anthracite coal. Most of the coal seams are affected by uncontrolled fires, and several high-temperature surface coal fires have been burning in the E and W parts of the coal field.

The Wuda Coal Field (latitudes 39°28′ to 39°34′, longitude 106°36′ to 106°40′) is located NE of the Helan Mountain range in a dessert-like environment with elevations ranging between 1100 and 1300 m asl. The coal bearing strata are composed of platform deposits of Upper Carboniferous and Lower Permian Taiyuan and Shanxi Formation. Twenty-four coal seams are exposed in a 10-km-long and 4-km-wide N–S striking syncline. In contrast to the Rujigou Coal Field, most of the coal fires occur underground and can be related to small-scale mining operations. The coal quality is in the range of medium volatile bituminous coal.

The coal layers of the two study areas in Xinjiang belong to Lower and Middle Jurassic lacustrine-fluvial deposits of the Tian Shan Mountains. The Tielieke Coal Field (latitudes 42°31′ to 42°50′, longitude 81°19′ to 81°34′) is part of the Southern Tian Shan Mountain Range. Mountaintops can reach up to 2750 m asl in the Tielieke area. Twelve coal seams with a cumulative thickness of up to 15 m are reported in the Jurassic Keselanuar Formation. The strike of the Tielieke strata is NW–SE following the general strike of the Tian Shan Mountains. Six coal seams are sufficiently thick to be mined. Coal seams are burning in large areas at and below the surface (Gielisch, 2002).

The Ke-er Jian Coal Field (latitudes 44°02′ to 44°10′, longitude 87°51′ to 88°48′) is located in the transition zone of the Tian Shan Mountains and the Turfan Depression in a hilly environment. The geological strata of the Ke-er Jian area are strongly folded and faulted. Tectonically, a northern anticline and a southern syncline can be subdivided. The coal-bearing strata belong to the Lower Jurassic Ba Dao and the Middle Jurassic Xi Shan Yao Formation. Three main coal layers are affected by several coal fires in this area (Gielisch, 2002).

3. Introduction to satellite remote sensing techniques applied

Within this study different satellite-based remote sensing techniques are synergistically combined to detect, analyze, and monitor coal seam fires. While some of the techniques are used for direct observation and detection of the fires (e.g., analysis of thermal imagery), other methods provide the crucially required reference data for geometric and radiometric correction of the satellite imagery [e.g., interferometrically derived digital elevation models (DEMs)] or allow for indirect observation of coal fires and their impact to the environment (e.g., detection of coal deposits, mapping of land cover, analysis of vegetation density or the estimation of surface subsidence rates by means of differential radar interferometry). The following section introduces methods applied in this study and demonstrates their application on a local and regional scale in northern China.

3.1. Digital elevation models from SAR interferometry

The German Remote Sensing Data Center (DFD) developed an interferometric processing system mainly designed for the operational derivation of digital elevation models (DEMs) from space borne synthetic aperture radar (SAR) systems such as European Space Agency (ESA) Remote Sensing Satellite (ERS), Shuttle Radar Topography Mission (SRTM) and Envisat Advanced Synthetic Aperture Radar (ENVISAT-ASAR) (Roth et al., 1998). It consists of a line of processors allowing the ingestion of different SAR input products at different preprocessing levels. The SAR processor (Eineder and Adam, 1997) generates the single look complex product (SLCI) from the annotated raw data and derives the intensity images, the coherence map, and the interferogram of the unwrapped phase from the SLCI. Geocoding and mosaicking of the large area satellite SAR coverages were performed by transforming the absolute phase values of the interferometric image pairs into elevation information and geocoding the individual DEMs. In a later step, these DEMs are mosaicked to large area elevation data sets and stored in a respective data management system. The base for this coal fire study consisted of SLCI standard products provided by the European Space Agency (ESA). The corresponding

raw data were acquired from the German Aerospace Center (DLR) mobile receiving station in Ulan–Bator as well as from the Beijing station. A special tie-pointing and adjustment procedure allowed an improvement of the initial geometry and phase measurements (Roth et al., 1999). After these adjustments were computed, the same imaging geometry was applied to geocode the elevation data as well as the radar images and the coherence data. The quality driving parameters with respect to the DEM generation were the time between the two acquisitions, imaging geometry, as well as the atmosphere.

In the current study the interferometric DEM generation was based on ERS data acquired during the so-called tandem mission of the ERS-1/2 satellites. Thus, the time gap between the acquisition of the interferometric pairs was as short as 24 h, providing optimal conditions for spaceborne repeat pass interferometry. The ERS pairs were selected with respect to optimum interferometric baseline. For the area of interest, the number of existing interferometric pairs was very limited; therefore, baseline lengths of 50–400 m were accepted. The baseline parameters could be improved by globally adjusting the DEM to a coarse digital reference elevation model allowing improved height estimation. Fig. 2 shows a DEM product for the Helan Shan Mountains derived from interferometry and fused with a coarse auxiliary DEM, where the ERS coverage was not sufficient.

The DEM's quality was ensured by the inspection of a difference image to the Global Land 1-km Base (GLOBE) DEM. In this way, detailed systematic errors like a phase ramp were avoided. Additionally overlapping areas between adjacent ERS pairs were compared to insure consistency. No systematic differences were detected. A detailed comparison with ASTER DEMs was not yet possible, because the currently available raw Advanced Spaceborne Thermal Emission and Reflection Radiometer (ASTER) DEMs (generated without additional tie-point control) showed large systematic errors.

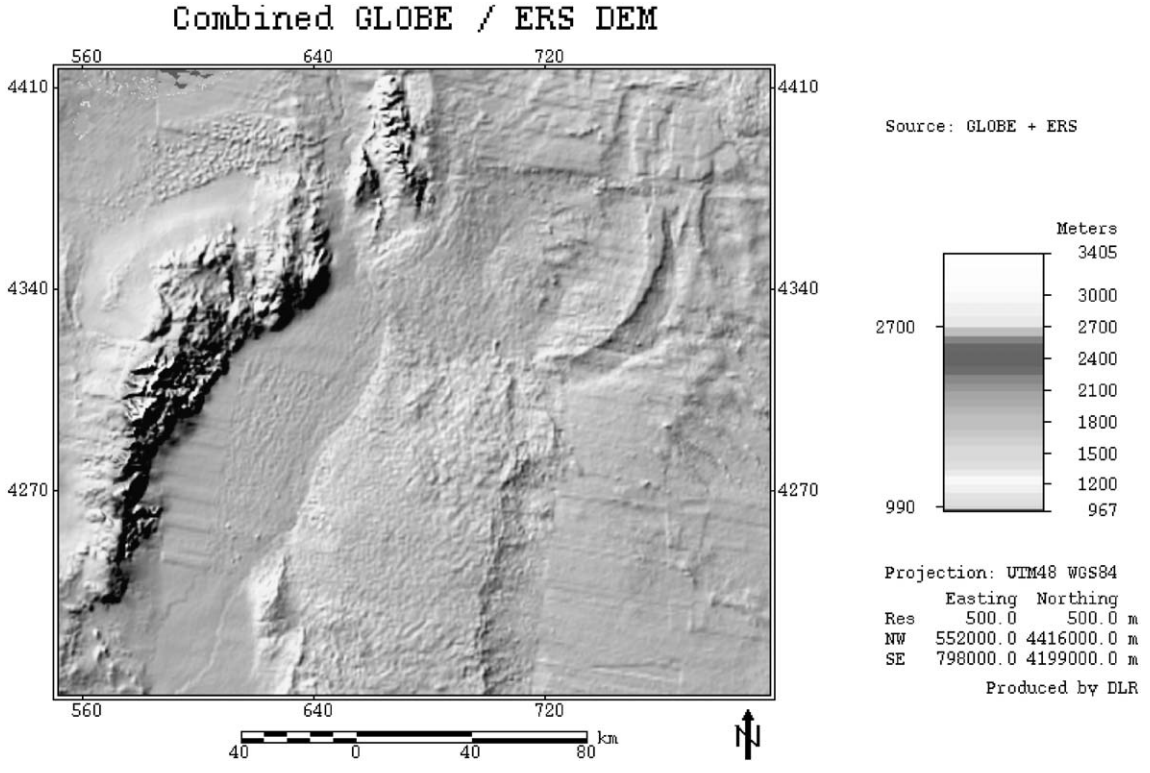

Fig. 2. Digital elevation model (DEM) derived by fusion of an interferometric mosaic and a coarse global digital elevation model.

All interferometric DEM products were stored in a geographical database. The database allowed geographical searches, status inspections, etc. In addition to the elevation model, a height error map, which is a mosaic of the intensity images, and the coherence map were stored in the database for combination with other remote sensing products and postprocessing. These DEMs provided a crucial base for several other methods of satellite data analysis. The most prominent ones were orthorectification and radiometric correction of optical and thermal satellite data, thermal modelling of solar effects to improve coal fire detection, GIS modelling of coal fire characterizations and input for differential interferometry.

3.2. Multispectral characterization of coal fire surface properties

Because it is difficult to obtain accurate and up to date large-scale topographic maps of remote areas in north China, a multispectral false color satellite map from Landsat-7 ETM data was produced for the Province of Ningxia. The satellite map gave an overview of the areas of interest with regard to coal fires in this region. Landsat-7 satellite data for the map was acquired during two DLR downlink campaigns with a mobile satellite receiving station in Ulan Bator, Mongolia. This data acquisition was complemented by scenes from the archives of the EROS Data Center operated by the US Geological Survey. Thus, it was possible to set up a Landsat-7 database that generated large area satellite maps for the Helan Shan region in Ningxia/Inner Mongolia and the coal fields of the province of Xinjiang in the North West. The satellite map served as the main orientation and reference source for planning and conducting of field work and ground inspections in the coal fields.

In addition, these optical satellite data were used to derive land cover classifications supporting the characterization of the environments of the coal fire and mining areas. Dominating surface types, vegetation patterns and agricultural structure, natural coal outcrops, coal piles, human-induced surfaces, and other relevant surface information were derived and used to understand and monitor environmental and human induced processes in coal fire regions.

A thorough preprocessing of satellite data was necessary to grant geometrically and radiometrically accurate results and allow for comparison of the products of different satellite data sets in time and space. To account for relief- induced object displacements, the satellite data were orthorectified with the digital elevation model generated from ERS SAR data. Because no maps were available for the large extent of Landsat-7 scenes, the ERS SAR amplitude data were used for the careful selection of ground control points of known location. The geometric correction was then performed using a nearest neighbor resampling algorithm. Geometric accuracy for the specific study areas was improved by using GPS reference points observed in the field. Thus, an overall geometric accuracy of less than one Landsat pixel (30 m) could be achieved. Without the addition of GPS reference points the broad scale geometric accuracy of the routinely processed Landsat-7 data was on the order of 50 m, which is a good result considering the extreme relief in the areas covered (Lunetta, 1999; Goward et al., 2001).

The data used for land cover classification was furthermore radiometrically corrected using the ATCOR 3 atmospheric correction model based on MODTRAN radiative transfer code (Richter, 1998, 2001). This allowed for approximating atmospheric conditions during the satellite overpass and scanning process and therefore to correct the scenes for atmospheric influences of water vapor, ozone, aerosol contents, and the atmospheric mass depending on terrain elevation. Furthermore, the data was topographically corrected to account for illumination changes resulting from differing sun-sensor-surface geometries (Song et al., 2001). The complete preprocessing sequence is shown in Fig. 3.

The spatial and radiometric corrections were followed by a supervised classification process based on the knowledge gained during fieldwork conducted in September 2002. For the classification, the widely applied maximum likelihood approach was used assigning each pixel the land cover class, which is most likely when comparing the pixel signature with the training signature of different land cover classes. Fig. 4 shows a classification for the Wuda coal mining area east of the Yellow River in southern Inner Mongolia.

Classifications for Wuda and Rujigou were evaluated based on ground truth data derived during a field visit in September 2002. Over 170 ground truth

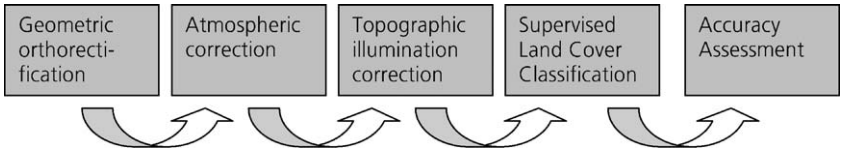

Fig. 3. Processing chain of Landsat-7 data.

polygons, between 10 m^2 and 1 km^2 in size, were identified and mapped. The results were ingested into a standard GIS and the digitally available polygons were then used to evaluate the thematic accuracy of the classification. Typical polygons included the classes of coal, coal waste, sand, sandstone, shale, sparse and dense vegetation, water, settlement, geologically mixed surfaces, carbonate rock, and carbonate rock quarries, among others. Overall accuracies exceeded 80%.

Classifications were also derived for the area of Rujigou, test sites in Xinjiang and the border surrounding the specific study areas. The classification scheme was adapted to the official legend of the Chinese Academy of Sciences to allow exchange and comparisons. Some work in the thermal related field of coal fire research can indirectly profit from the land cover classifications. Surface maps of different land cover types or geologic classes can be transferred into thermal emissivity maps or thermal inertia maps assigning a physical value to each land cover class supporting the calibration of the thermal data.

To keep an overview of the large amount of satellite scenes processed, a GIS database was implemented to organize and provide an overview of data available within this study. This database is

Satellite Image, Landsat-7 ETM+

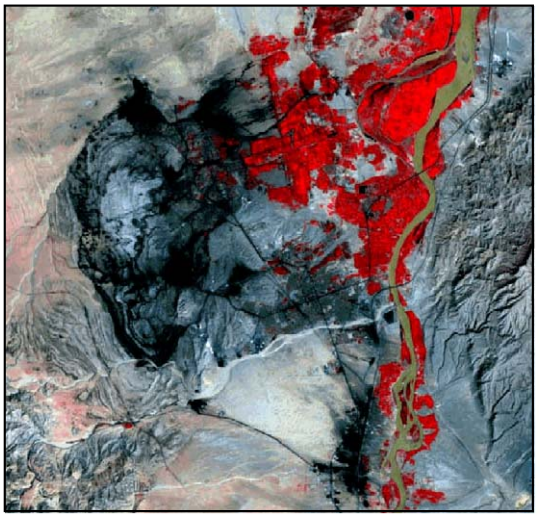

False Color near Infrared Composite (bands 4-3-2) for the coal mining of Wuda (vegetation appears red) size of subset approximately 30*40km≤

Classification Result

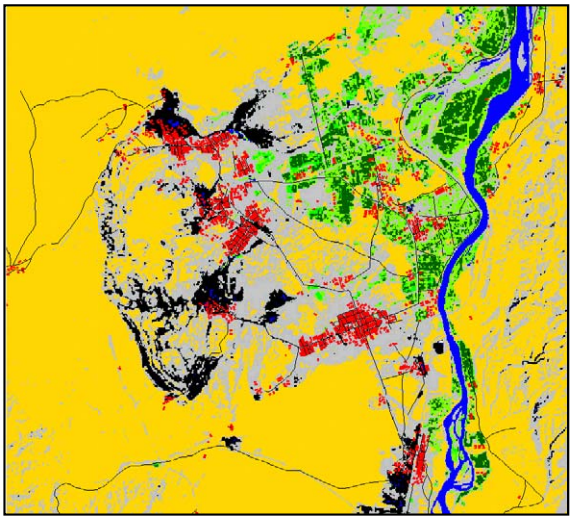

Black: coal, **Red**: settlement, **Blue**: water, **Gray**: coal related surfaces and shadows, **Light Green**: sparse vegetation, **Dark Green**: dense vegetation, **Yellow**: Sand & geologically mixed surfaces

Fig. 4. Land cover classification for the coal mining area of Wuda.

set up in ArcMap giving the option to visualize the available daytime and nighttime Landsat-7 frames, Bispectral IR Detection (BIRD) and ASTER data, the available extent of the ERS digital elevation model, the coverage with topographic maps, the exact location of our test areas as well as further vector features like province borders, rivers, streets and other infrastructure.

3.3. Spaceborne thermal analysis of coal fires

Thermal satellite imagery has been used to delineate and analyze coal fires (e.g., Mansor et al., 1994; Prakash et al., 1995, 1997, 1999; Reddy and Bhattacharya, 1995; Zhang et al., 1997a,b; Zhang, 1998; Vekerdy et al., 1999). Within this study, operational algorithms for large-scale spaceborne thermal coal fire delineation and characterization were developed. For this purpose, the following satellite sensors were applied, either for their high spatial or for their high spectral resolution in the infrared part of the electromagnetic spectrum: Moderate-resolution Imaging Spectroradiometer (MODIS), BIRD, ASTER and ETM. The MODIS sensor has several thermal infrared (TIR) bands with a spatial resolution of 1 km. DLR's small satellite (BIRD), an experimental fire remote sensing satellite launched in October 2001, has three nadir looking bands at the wavelength of 0.84–0.90 μm [near infrared (NIR)], 3.4–4.2 μm [middle infrared (MIR)] and 8.5–9.3 μm [thermal infrared (TIR)] with a pixel spacing of 185 m (Briess et al., 2003). ASTER spans the 8–12 μm region with five contiguous bands at 90-m resolution. ETM has one thermal band (10.4–12.5 μm) with a 60-m spatial resolution.

Automated fire detection algorithms have been developed for GOES VAS (Prins and Menzel, 1994), AVHRR (Lee and Tag, 1990; Kaufman et al., 1990a,b; Setzer and Pereira, 1991), MODIS (Kaufman et al., 1998) and BIRD (Zhukov and Oertel, 2001) data. The algorithms are based on the assumption that an image pixel affected by fire is characterized by an enhancement of brightness temperature and an enhanced brightness temperature difference between a short wave or midwave infrared channel and a long-wave thermal infrared channel relative to the surrounding nonfire pixels. The later is caused by the fact that the hotter fire portion within an image pixel will contribute more to the pixel averages radiance observed in the short and midwave infrared than in the longer wavelengths (Planck's law).

Multispectral infrared data sets allow a quantitative estimation of the effective coal fire temperature and area. Assuming that an image pixel always contains background and fire information, the fire temperature and area can be determined using the bispectral technique (Dozier, 1981). This technique is based on the concept, that the contribution of the hotter portion within one pixel is different at different wavelengths. Considering the thermal radiance values of two channels in a pair of nonlinear equations and using the background radiance value of the surrounding nonfire pixels as background radiation the effective fire temperature and area can be determined. In addition the bispectral technique allows an estimation of the radiative energy release of a coal fire relative to the background as $P_F=\sigma(T_F^4\text{-}T_{BG}^4)A_F$, where σ is the Stefan–Boltzmann constant, T_F is the effective fire temperature, T_{BG} is the background temperature, and A_F is the effective fire area.

Application of these detection criteria for MODIS imagery in the Ningxia and Xinjiang coal fires study area have not shown any coal fire related thermal anomalies, yet. Nighttime and daytime data as well as imagery of different seasons have been examined. While spatial resolution of the MODIS data seems to be too coarse to detect coal fires in a direct way, ASTER, BIRD and ETM data have shown a good potential to delineate coal fires. BIRD and ETM data processing is discussed in detail in the following two sections.

3.3.1. BIRD data analysis

Starting from the end of January 2002, BIRD has been used to image the coal field areas in Ningxia and Xinjiang. Periodic BIRD observations were performed over the Rujigou and Wuda Coal Fields in the Helan Shan area also. The remote coal fire detection results in these areas could be verified by a field survey in September 2002. Coal seam fires are detected and analyzed using the BIRD hotspot detection algorithm (Zhukov and Oertel, 2001) that includes the following tests:

- adaptive MIR thresholding to detect potential hot pixels,
- NIR thresholding to reject strong sun glints,

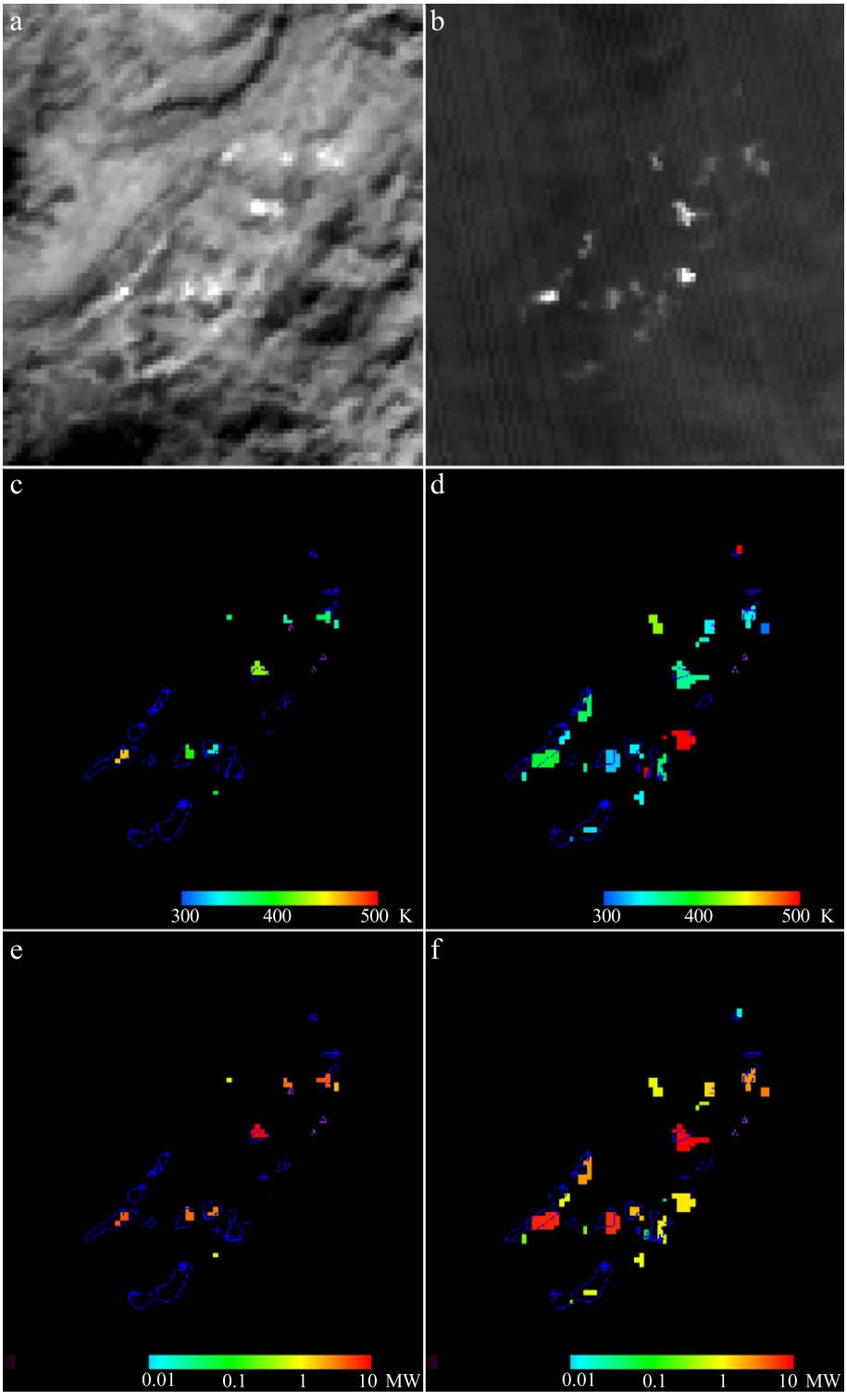
a
b
c
300 400 500 K
d
300 400 500 K
e
0.01 0.1 1 10 MW
f
0.01 0.1 1 10 MW

- adaptive MIR/NIR radiance ratio thresholding to reject weaker sun glints, clouds and other high-reflective objects,
- adaptive MIR/TIR radiance ratio thresholding to reject warm surfaces,
- consolidation of adjacent hot pixels in hot clusters (hotspots) and estimation of hotspot characteristics, the effective fire temperature and area, and radiative fire energy release using the bispectral technique (Dozier, 1981).

The fire detection thresholds were adapted to the median background characteristics of the specific test sites and selected high enough to provide false alarm rejection in all the BIRD images of these test sites acquired in various seasons.

Fig. 5 shows examples of coal fire detection in day and nighttime BIRD images over the Rujigou Coal Field. The daytime MIR image (Fig. 5a) shows a few bright spots that allow detection and retrieval of their effective fire temperature and energy release (Fig. 5c and e). They can be associated with stronger coal seam fires (and in one case with an industrial chimney) mapped on ground within a few days after the BIRD data were taken. However, some of the weaker fires (verified during ground inspection in September 2002) could not be detected during the day due to masking effect of the reflected solar radiation and of background temperature variations. The nighttime BIRD MIR image data (Fig. 5b), in spite of a moderate signal-to-noise ratio, allowed the recognition of most of the verified (September 2002) weaker coal fire anomalies and the estimation of their characteristics (Fig. 5d and f). The thresholds were adapted to the nighttime observation conditions.

The effective temperature of most of the fire-affected surfaces as retrieved by the bispectral technique was in the range of 300–400 K, which is significantly lower than typical temperatures in the burning core of coal fires. This indicates that the radiation of the heated surfaces around the coal fires dominated the signals of the detected hot spots. The radiative energy release of the coal seam fires ranges from ~0.01 MW for the weakest detected fires at nighttime up to ~10 MW for the strongest fires. Thus, BIRD has proven its potential for quantitative coal fire monitoring during the day. Night monitoring proved to have greater sensibility due to less variation in background temperature.

3.3.2. ETM data analysis

ETM data sets from 1999 to 2002, including the Rujigou and Wuda Coal Fields, were analyzed. Ground verification was carried out in September 2002. A listing of ETM scenes used for this study is given in Table 1. Because most of the coal fires showed up in one ETM band (TIR channel), an operative coal fire detection algorithm for ETM had to make use of a single band concept. Here, a statistical method was developed. Thresholds to distinguish coal fire and noncoal fire pixels were derived on a pixel-by-pixel basis using a moving window technique, thus allowing coal fire detection in large, thermally inhomogeneous areas.

Fig. 6 shows examples of detected 'warm spots' on ETM nighttime imagery of the Wuda Coal Field. Thermal nighttime anomalies (red) are plotted on optical daytime data. Thermal anomalies within the Wuda Syncline (white outline area) can be related to coal fires. False alarms in the observed nighttime ETM image are caused by industries, water and sun-heating effects remaining from daytime solar irradiation, or by inhomogeneous cooling during the nighttime.

A quantitative characterization of coal fires using ETM satellite imagery requires data calibration, thus digital numbers (DN) from satellite data have to be converted to radiance values and at-satellite brightness temperature using sensor calibration constants and Planck's equation. To obtain land surface temperature

Fig. 5. Coal fire detection and quantitative characterisation in the BIRD images obtained on 21 September 2002 at daytime (left) and on 16 January 2003 at night (right). (a) Daytime MIR image; (b) nighttime MIR image; (c) effective fire temperature of detected hotspots at daytime (~11 am local time); (d) effective fire temperature of detected hotspots at night (~11:00 pm local time); (e) radiative energy release of detected hotspots at daytime; (f) radiative energy release of detected hotspots at night. Blue contours and crosses show location of coal seam fire verified on ground in September 2002, while purple triangles show location of industrial chimneys.

Table 1
Listing of satellite images used in this study

Sensor	Path/Row	Acquisition date
ETM (Thermal Analysis)	129/33	2002/09/21 (day)
	226/221	2002/09/28 (night)
	129/33	2002/10/04 (day)
	226/221	2002/09/25 (night)
ETM (Landuse Analysis)	129/33	2002/09/21 (day)
	129/33	1999/08/12 (day)
BIRD		2002/01/31 (daytime)
		2002/02/06 (daytime)
		2003/03/22 (daytime)
		2002/08/06 (daytime)
		2002/09/21 (daytime)
		2002/10/10 (daytime)
		2002/11/27 (night-time)
		2003/01/16 (night-time)

values, it is necessary to correct at-satellite brightness temperatures for atmospheric effects and land surface emissivity. A conversion of DN to brightness temperature as well as an atmospheric and surface emissivity correction is included in the ATCOR 3 model (Richter, 1998). The ATCOR 2 model was used to correct ETM daytime and nighttime data sets acquired during September 2002 over the Helan Shan study area. A comparison of remotely sensed water temperatures and on-ground measurements has shown a maximum deviation of 1.3 K for ETM.

The bispectral technique (Dozier, 1981) can not be applied when thermal anomalies do not exhibit elevated brightness temperature values in at least two infrared bands, which is often the case with ETM imagery. Coal fires are normally not hot enough to be picked up in the short-wave infrared wavelengths, and therefore only show enhanced brightness temperatures in the thermal infrared channel. In order to quantify these fire observations, the temperature difference of the coal fire pixels relative to the surrounding background pixel was computed. Around each potential fire pixel, the mean background value was calculated in a 2×2 up to 20×20 moving window, until at least six nonfire pixels are available for the computation. If less than six pixels were included in the 20×20 pixel box, the central pixel was expected not to be affected by fire. Although fire area and temperature can not be

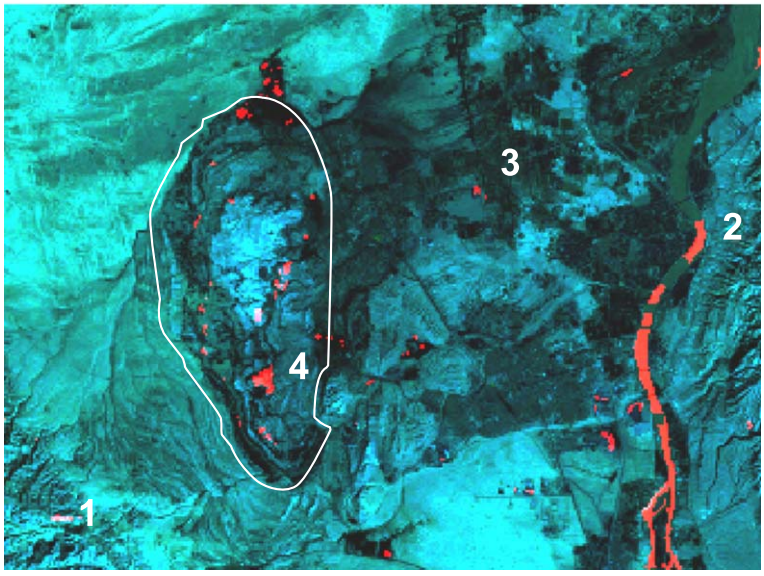

Fig. 6. ETM thermal nighttime anomalies (red) of Wuda Coal Field plotted on ETM optical daytime data. The white line marks the Wuda Coal Field. Thresholds to distinguished coal fire and noncoal fire pixels are derived on a pixel-by-pixel basis from a spatial window about each pixel. False anomalies are related to water surfaces (2), industries (3) and sun surfacing slopes (1). Daytime image: ETM, 2002/10/04, Nighttime image: ETM, 2002/09/25.

determined from satellite data alone in the case of ETM, coal fires over different backgrounds can be compared and classified into different groups according to their temperature difference relative to the background.

Fig. 7 shows examples of 'warm spot' detection in ETM thermal images of the Rujigou Coal Field. The spatial subset of the images corresponded to the BIRD image in Fig. 5. Thermal anomalies were derived using fixed brightness temperature thresholds at 306 K (daytime images) and 283 K (nighttime images). Temperature differences of detected anomaly pixels relative to the surrounding background are shown in Fig. 7c and d.

Although many coal fires show enhanced brightness temperature values relative to the background in the ETM thermal images (Fig. 7a and b), a coal fire detection algorithm using fixed brightness tem-

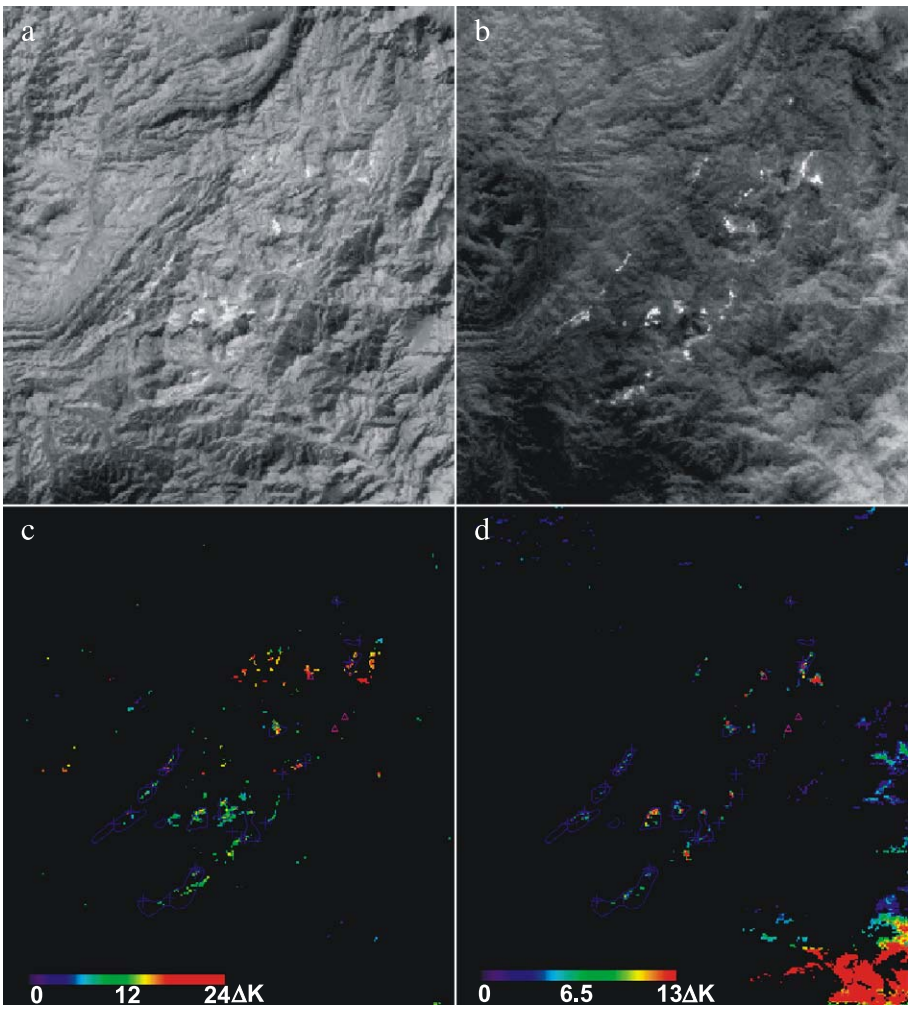

Fig. 7. 'Warm spot' detection and quantitative characterisation in the ETM images obtained on 21 September 2002 at daytime (left) and on 28 September 2002 at nighttime (right). (a) Daytime TIR image; (b) nighttime TIR image; (c) temperature difference of anomaly pixel according to surrounding nonanomaly pixels (~ 11 am local time); (d) temperature difference of anomaly pixel according to surrounding nonanomaly pixels (~ 11:00 pm local time). Blue contours and crosses show location of coal seam fire verified on ground in September 2002, while purple triangles show location of industrial chimneys.

perature underestimates the coal fire area (Fig. 7c and d). In addition, many false anomalies can be observed in daytime as well as in nighttime ETM images. The false anomalies shown in Fig. 7c and d can be related to topographic and solar irradiation effects. Differences in temperature of coal fire pixels relative to the surrounding background pixels are higher during the day due to a general higher background variation of the observed daytime image.

These large variations, even observed in nighttime imagery, lead to the conclusion that in order to automatically detect coal fires using ETM imagery, a sun correction method has to be included in an automatic detection algorithm. Experiments with DEM approaches and models to reject strongly heated surfaces, based on optical channels, showed promising results.

3.4. Experiments on land surface subsidence using differential SAR interferometry

As a further method to remotely study and analyze coal fires, the potential of differential SAR interferometry (DINSAR) for the assessment of land surface subsidence resulting from coal fires was evaluated. The method exploits the coherence properties of spaceborne synthetic aperture radar (SAR) sensors such as the ERS-1/2 Missions of ESA. Differential interferometric techniques assess the phase differences between two or more interferograms resulting from at least two pairs of satellite overpasses. From these differential interferograms, the velocity of ground movements on the order of cm per year can be derived (Massonnet and Feigl, 1998). Where it is possible to link observed ground movements to coal fires burning in the underground,

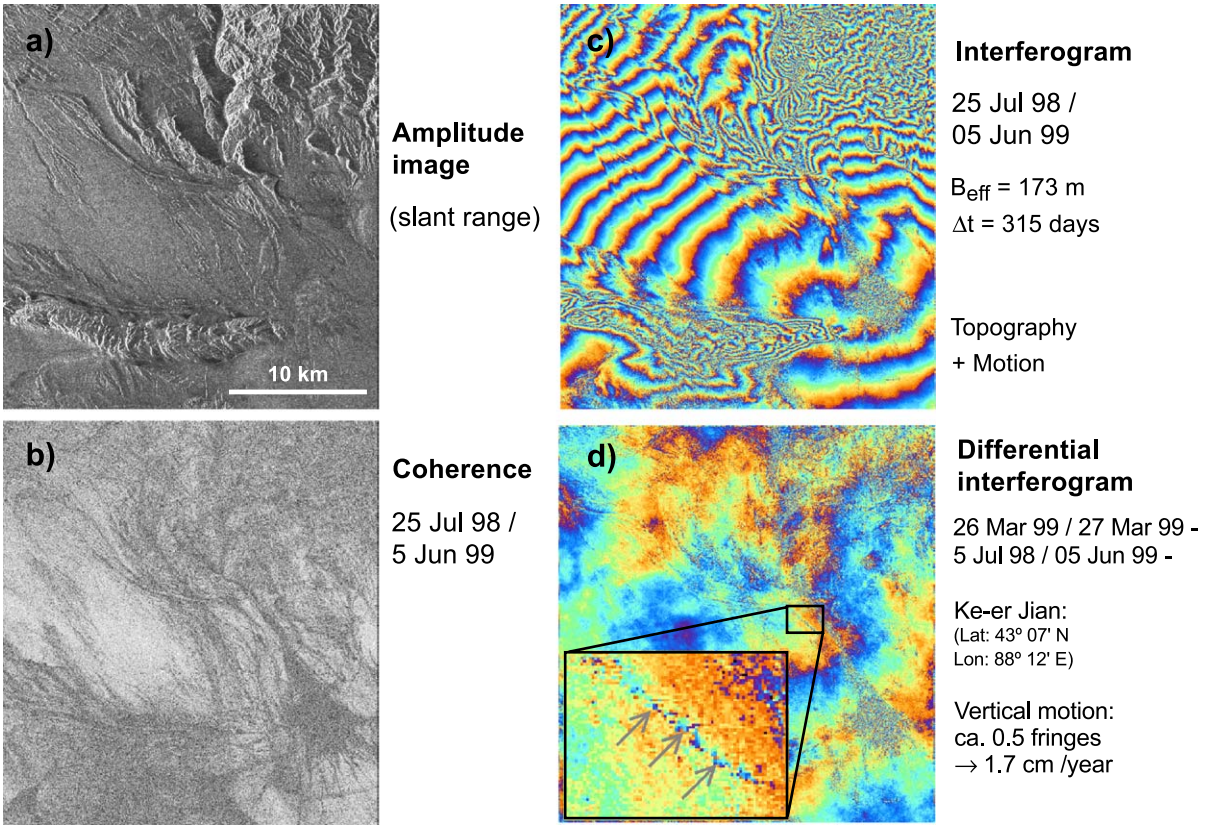

Fig. 8. Analysis of land surface subsidence in the Ke-er Jian Coal Field in Xinjiang Province, Northwest China: radar amplitude (a), coherence of one interferometric pair (b), phase interferogram (c) and differential interferogram (d).

this method provides additional information for analyzing and monitoring coal fires from space. The processing of SAR data is partially linked to the methods for interferometric derivation of the DEMs because it uses the same type of data source and some of the basic preprocessing steps.

In order to evaluate the general feasibility of the DINSAR techniques for coal fire detection and analysis a data stack of a 16 ERS-1/2 SAR, scenes were processed for a study area in Xinjiang, Northwest China, and suitable combinations of interferometric pairs were analyzed. After removing the first-order phase effects of the ''flat earth'' and the second-order effects of the terrain, the phase differences resulting from local ground movements over the coal fires zone in the Ke-er Jian fire zone could be identified and quantified. Thus, the general feasibility to detect land surface subsidence in the context of coal seam fires in North China using classical differential SAR interferometry was demonstrated.

Fig. 8 shows the typical products used in interferometric analyses. As a first step, the radar raw data stream was processed to derive the single look complex radar image containing the amplitude and phase information. In a second step, suitable interferometric pairs were selected covering appropriate time intervals and showing sufficient coherence for further analysis. Third, the interferograms were computed and finally, in order to eliminate the topographic phase, the differential interferogram was derived and analyzed for ground movements and possible land subsidence. In the example shown in Fig. 8, one can clearly identify the linear subsidence features along a coal fire front in the Ke-er Jian Coal Field in Xinjiang Province. Subsidence effects on the order of 1.7 cm/year can be identified along the coal fire front. It has to be noted that at this stage of the processing it is not possible to differentiate land subsidence affects resulting from coal fires and those resulting from ordinary mining activities in the area. It is subject of further investigations on how these effects can be separated. Most likely this will be possible by correlation with geometrical features and properties of the different subsidence effects. Also in this case, a synergistic analysis combining interferometric and thermal analysis will help to distinguish between these effects.

Another interesting finding of the analysis carried out so far was the high radar coherence observed in the test area. The dry desert-type environment, experiencing extremely little rain, resulted in very stable backscatter properties of the land surface over time, thus allowing even standard differential interferometry to be successful in the area. In areas where such stable conditions cannot be found, such analysis would be very difficult or even impossible.

It is important to note that not all phase effects left in the differential interferogram can be related to land subsidence. These are typical third-order effects resulting from insufficient estimation of the baseline (on the orders of mm to cm) (Zebker et al., 1994) or the subtle influence of changing atmospheric conditions between the interferograms (Hanssen, 1998). Thus, it can be understood that further methodological developments are required to semi-automatically or automatically quantify the land subsidence component of the phase differences resulting from coal fires.

4. Results of the comparison with field surveys and reference data

For better interpretation and verification of the different remote sensing products, results were extensively compared with field surveys and reference data. In the case of the DEMs, this comparison was done with locally available topographic maps, GPS measurements, and a coarse reference DEM. For those parts of the test areas where topographic maps were available, the comparison showed satisfactory agreement. In areas where the used interferometric image pairs showed poor radar coherence, the phase-related elevation errors were larger than in the areas of high coherence. As another test, the interferometrically derived DEMs were compared to the GLOBE reference DEM. Thus, it was possible to verify and document the overall consistency with respect to the general location accuracy in latitude and longitude as well as in absolute height estimation. As a third check, the overall image geometry of the satellite products was cross-checked with local GPS measurements of prominent landmarks such as roads, crossroads, bridges or railway lines.

In an extensive ground truthing campaign in September 2002, reference samples of the typical land cover features in the study areas were mapped and later used for calibration as well as validation of the satellite data analysis. For this purpose, large homogenous areas of the representative land cover types were mapped in the study regions of the Helan Shan Mountains and geometrically referenced by GPS measurements. While the discrimination of coal seam outcrops, coal processing or piling areas as well as vegetated/agricultural land was very stable, due to the large spectral contrast to the surrounding dessert type environments, the separation of different geological features proved to be more critical. For the sake of robustness of the classification approach, the geological features were therefore aggregated in a land cover class "sand and geologically mixed surfaces".

With respect to thermal detection and analysis of the fires by means of infrared satellite imagery, the fire areas in the respective study regions were mapped and characterized in terms of thermal surface properties using GPS measurements, radiant thermometers, and local mine layout charts. Thus, all the fires that showed thermal surface anomalies in the region could be surveyed and mapped for comparison with the satellite observations. Furthermore, large-scale industrial complexes such as cement or coking plants as well as steel factories in the regions were located and mapped in order to check for false alarms in the coal fire detection algorithms caused by the thermal emissions of such industries. Results of the comparison show that even very subtle thermal anomalies, warm spots, are detectable in the thermal channels of the ETM sensor. Of course, these detections will be more reliable the warmer/hotter or larger an anomaly is. In the study area, many fires were found to span more than one ETM image cell (60×60 m) and could therefore be picked up very effectively. While the daytime thermal imagery from ETM (taken at 10:30 am local time) showed severe influence of solar heating and surface characteristic effects, sometimes even masking the coal fire related anomalies, the thermal nighttime imagery of ETM showed much smaller, although still noticeable, solar heating disturbances. In the BIRD satellite data, having a spatial sampling of 185×185 m, the detection and quantification of larger near-surface fires proved to be possible using the bispectral technique. During nighttime data takes, the BIRD system could even pick up some "warm" anomalies, which proved to be impossible during daytime due to the solar-heating effects and the small spatial extent of these warm spots.

For the verification of the first experimental results of land surface subsidence mapping using differential radar interferometry over coal fire areas, the derived vertical displacements maps over the test area in Ke-er Jian, Xinjiang Province was compared with GPS surveys of the respective coal fire locations. The comparison showed good geometrical coincidence; however, so far no comparison with direct field measurements of vertical subsidence rates could be conducted. It will be subject of further research to measure such subsidence rates in the Chinese coal fire areas and establish these quantitative comparisons.

5. Conclusions

In this study, it could be shown how different spaceborne remote sensing techniques could be synergistically applied to detect, map, and analyze coal fires and their surroundings in northern China in a quantitative way. While some of the methods can be considered to be in a mature state, such as the derivation of DEMs from interferometric radar data for example, other methods, such as the semiautomatic coal fire detection using optical or thermal satellite data, or the mapping of land surface subsidence have to be considered preoperational or experimental. Currently, the different methods used in this study are being combined in a semiautomatic way to exploit their full synergistic potential. It will be subject of further work and research to improve the robustness of these analysis and detection techniques and to further automate the processing. Thus, it will be possible to meet the challenges of integrating these methods into an operational coal fire detection and monitoring system, allowing to routinely observe, more efficiently fight, and avoid such fires. While for now, the methods have proven to be able to detect and analyze mature and developed coal fires, further research will be required to refine these methods for detecting very small and young fires and thus move from inventorying and analyzing the fires to early warning and avoidance. A further challenge will be the extension of these methods

from regional to continental or even global scales, and applying them under different environmental and geological conditions. Especially when it comes to large area or very frequent analysis, inventory, or monitoring of coal fires in remote or inaccessible regions such spaceborne coal fire monitoring methods can fully develop their proven potential.

Acknowledgements

This work was funded by the German Ministry of Education and Research (BMBF). The authors would like to thank the Chinese Ministry for Science and Technology, the National Remote Sensing Centre of China, Shenhua Coal Group and the Engineers of Wuda, GulaBen and Rujigou Coal Fields for the kind cooperation and support of this research work. Furthermore, we want to thank the Deutsche Montantechnik GmbH for providing the GPS reference data for the Ke-er Jian Coal Field in Xinjiang. Finally, we would like to thank Tammy P. Taylor of Los Alamos National Lab, NM and Donald C. Rundquist of the University of Nebraska, Lincoln for carefully reviewing the manuscript.

References

Briess, K., Jahn, H., Lorenz, E., Oertel, D., Skrbek, W., Zhukov, B., 2003. Fire recognition potential of the bi-spectral infrared detection (BIRD) satellite. International Journal of Remote Sensing 24 (4), 865–872.

Dozier, J., 1981. A method for satellite identification of surface temperature fields of subpixel resolution. Remote Sensing of Environment 11, 221–229.

Eineder, M., Adam, N., 1997. A flexible system for the generation of interferometric SAR products. Proceedings IGARSS'97 on CD-ROM, E06-02, IEEE, Piscataway, NJ, USA.

Gielisch, H., 2002. Statusbericht zum GTZ-Project: Löschung von Kohlebränden in der VR China. Unpublished.

Goward, S.N., Masek, J.G., Williams, D.L., Irons, J.R., Thompson, R.J., 2001. The Landsat 7 mission. Terrestrial research and applications for the 21st century. Remote Sensing of Environment, vol. 78, pp. 3–12.

Hanssen, R., 1998. Atmospheric Heterogeneities in ERS Tandem SAR Interferometry. Delft Univ. Press, Delft, the Netherlands.

Kaufman, Y.J., Setzer, A., Justice, C., Tucker, C.J., Pereira, M.C., Fung, I., 1990. Remote sensing of biomass burning in the tropics. In: Goldammer, J.G. (Ed.), Fire in the Tropical Biota: Ecosystem Processes and Global Challenges, pp. 371–399. Springer-Verlag, Berlin.

Kaufman, Y.J., Tucker, C.J., Fung, I., 1990. Remote sensing of biomass burning in the tropics. Journal of Geophysical Research 95 (D7), 9927–9939.

Kaufman, Y.J., Justice, C.O., Flynn, L.P., Kendall, J.D., Prins, E.M., Giglio, L., Ward, D.E., Menzel, W.P., Setzer, A., 1998. Potential global fire monitoring from EOS-MODIS. Journal of Geophysical Research 103, 215–238.

Lee, T.F., Tag, P.M., 1990. Improved detection of hotspots using the AVHRR 3.7 m channel. Bulletin of the American Meteorological Society 71 (12), 1722–1730.

Lunetta, R.S., 1999. Applications, project formulation, and analytical approach. In: Lunetta, R., Elvidge, C.D. (Hrsg.), Remote Sensing Change Detection, London, S.1–14.

Mansor, S.B., Cracknell, A.P., Shilin, B.V., Gornyi, V.I., 1994. Monitoring of underground coal fires using thermal infrared data. International Journal of Remote Sensing 15, 1675–1685.

Massonnet, D., Feigl, K., 1998. Radar interferometry and its application to changes in the Earth's surface. Reviews of Geophysics 36 (4), 441–500.

Prakash, A., Saraf, A.K., Gupta, R.P., Dutta, M., Sundaram, R.M., 1995. Surface thermal anomalies with underground fires in Jhahra coal mine, India. International Journal of Remote Sensing 16, 2105–2109.

Prakash, A., Gupta, R.P., Saraf, A.K., 1997. A Landsat TM based comparative study of surface and subsurface fires in the Jharia Coalfield, India. International Journal of Remote Sensing 18, 2463–2469.

Prakash, A., Gens, R., Vekerdy, Z., 1999. Monitoring coal fires using multi-temporal nighttime thermal images in a coalfield in North-west China. International Journal of Remote Sensing 20, 2883–2888.

Prins, E.P., Menzel, W.P., 1994. Trends in South American Biomass Burning Detected with the GOES Visible Infrared Spin Scan Radiometer Atmospheric Sounder from 1983–1991. Journal of Geophysical Research, 99 (16), 719–16, 735.

Reddy, C.S.S., Bhattacharya, A., 1995. Use of GPS for ground truth data collection and its integration with RS and GIS: a case study with reference to the mine fire mapping in Jharia, Bihar state, India. Asian-Pacific Remote Sensing Journal 7, 155–158.

Richter, R., 1998. Correction of satellite imagery over mountainous terrain. Applied Optics 37 (18), 4004–4015.

Richter, R., 2001. Atmospheric and Topographic Correction: Model ATCOR 3. Unpublished User Handbook.

Roth, A., Knöpfle, W., Hubig, M., Adam, N., 1998. Operational interferometric SAR products. Proceedings IGARSS'98, vol. 1. IEEE, Piscataway, NJ, USA, pp. 324–326.

Roth, A., Knöpfle, W., Rabus, B., Gebhardt, S., Scales, D., 1999. GeMoS—a system for the geocoding and mosaicking of interferometric digital elevation models. Proceedings IGARSS'99, vol. 1. IEEE, Piscataway, NJ, USA, pp. 631–633.

Setzer, A.W., Pereira, M.C., 1991. Amazonia biomass burnings in 1987 and an estimate of their tropospheric emissions. Ambio 20 (1), 19–22.

Song, C., Woodcock, C.E., Seto, K.C., Lenney, M.P., Macomber, S.A., 2001. Classification and change detection using Landsat TM data: when and how to correct atmospheric effects? Remote Sensing of Environment, vol. 75, pp. 230–244.

Vekerdy, Z., Prakash, A., Gens, R., 1999. Data integration for the study and visualisation of subsurface coal fires. Proceedings of the 13th International Conference on Applied Remote Sensing, 1–3 March, 1999. Vancouver, Canada. ERIM, Ann Arbor, MI, USA, pp. II-150–II-151.

Zebker, H., Werner, C., Rosen, P., Scott, H., 1994. Accuracy of topographic maps derived from ERS-1 interferometric radar. IEEE Transactions on Geoscience and Remote Sensing 32 (4), 823–836.

Zhang, X., 1998. Coal fires in Northwest of China, detection, monitoring, and prediction using remote sensing data. PhD thesis, ISBN 90-6164-144-6.

Zhang, X., van Genderen, J.L., Kroonenberg, S.B., 1997. A method to evaluate the capability of Landsat-5 TM band 6 data for subpixel coal fire detection. International Journal of Remote Sensing 18, 3279–3288.

Zhang, X., Cassells, C., van Genderen, J.L., 1997. Mapping underground coal fires using remote sensing and GIS techniques. Xth International Congress of the International Society for Mine Surveying, Fremantle, Western Australia, 2–6 November 1997.

Zhukov, B., Oertel, D., 2001. Hot Spot Detection and Analysis Algorithm for the BIRD Mission, Algorithm Theoretical Basic Document (ATBD). DLR, Berlin, Germany.